THE JOURNAL OF PHYSICAL CHEMISTRY C

ARTICLE

pubs.acs.org/JPCC

Enhanced Responsivity of Highly Spectrum-Selective Ultraviolet Photodetectors

Pei-Nan Ni,[†,‡] Chong-Xin Shan,[*,†] Shuang-Peng Wang,[†] Bing-Hui Li,[†] Zhen-Zhong Zhang,[†] Dong-Xu Zhao,[†] Lei Liu,[†] and De-Zhen Shen[†]

[†]State Key Laboratory of Luminescence and Applications, Changchun Institute of Optics, Fine Mechanics and Physics, Chinese Academy of Sciences, Changchun 130033, China

[‡]Graduate University of Chinese Academy of Sciences, Beijing 100049, China

ABSTRACT:

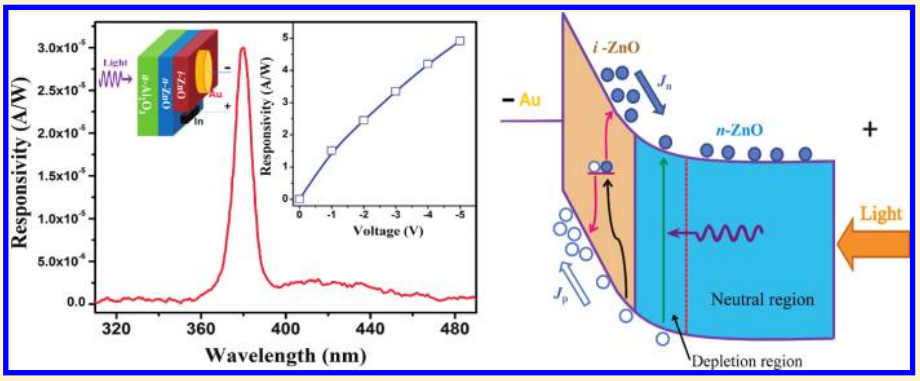

Highly spectrum-selective photodetectors have been proposed and fabricated from the *i*-ZnO/*n*-ZnO structure. In this structure, the *n*-ZnO layer acts as a "filter" that filtrates out the short-wavelength photons to ensure the high spectrum selectivity of the photodetector. Meanwhile, the *i*-ZnO layer acts as a "multiplier" in which photogenerated carriers can be multiplied via an impact ionization process. In this way, photodetectors with their response width of only 9 nm have been obtained, and the responsivity of the photodetectors can reach 4.91 A/W at −5 V bias, corresponding to a quantum efficiency of 1600%. The results reported in this paper may provide a general route to high-performance, highly spectrum-selective photodetectors.

INTRODUCTION

Ultraviolet (UV) photodetectors have received more and more attention in recent years due to their potential applications in a variety of fields including flame sensing, missile plume detection, medical diagnostics, chemical analysis, and advanced optical communications, etc.[1−4] For practical application consideration, UV photodetectors with better performance such as high sensitivity, good reliability, low fabrication cost, long lifetime, and lightweight are highly desired. Zinc oxide (ZnO) has been widely regarded as a promising material for UV photodetectors due to its large bandgap and high photoconductance.[5−8] Compared with other wide bandgap semiconductors, ZnO has many unique properties that are attractive for photodetectors, such as high saturation drift velocity,[9] high radiation resistance,[10] abundance, and low price, etc. These properties make ZnO-based UV photodetectors have various figure-of-merits such as high responsivity, low cost, long lifetime, and the ability to operate in a harsh environment.

It is well-known that, since photons with their energy larger than the bandgap of ZnO will be absorbed and contribute to the response, ZnO-based photodetectors usually show response to a broad spectrum region shorter than 380 nm;[11−15] namely, their spectrum selectivity is quite poor. For some practical applications where a very narrow spectrum range will be monitored, photodetectors with high spectrum selectivity are greatly desired. To achieve this purpose, an extra optical filter is traditionally required, which will definitely increase the cost of the photodetectors and degrade their usefulness. To avoid this disadvantage, we have proposed a highly spectrum-selective photodetector based on the *n*-ZnO/*p*-GaN heterojunction, in which GaN with a larger bandgap than ZnO acts as a "filter" to diminish the response to short-wavelength photons.[16] Later on, a report also demonstrated spectrum-selective photodetectors by employing a wider bandgap semiconductor as a "filter".[17] Nevertheless, since the filter will inevitably reduce the response of the photodetector, the performance of these photodetectors is usually below expectations.

In this paper, UV photodetectors with high spectrum selectivity and high responsivity have been proposed and fabricated, which are realized in insulating ZnO (*i*-ZnO)/*n*-ZnO structure.

Received: November 15, 2011
Revised: December 10, 2011
Published: December 10, 2011

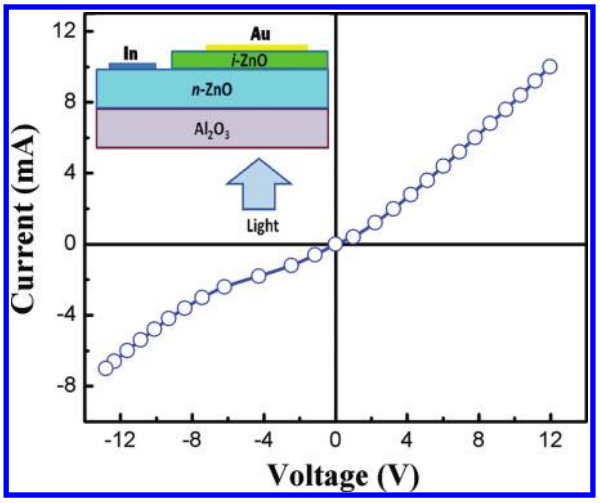

Figure 1. $I-V$ characteristic of the i-ZnO/n-ZnO structure. The reverse bias is defined as the negative voltage applied on Au contact. The inset shows the schematic structure diagram of this structure.

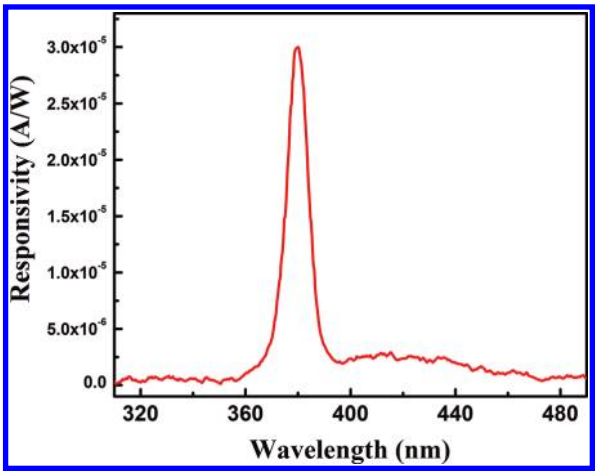

Figure 2. Room-temperature response spectrum of the photodetector under back-illumination at 0 V bias.

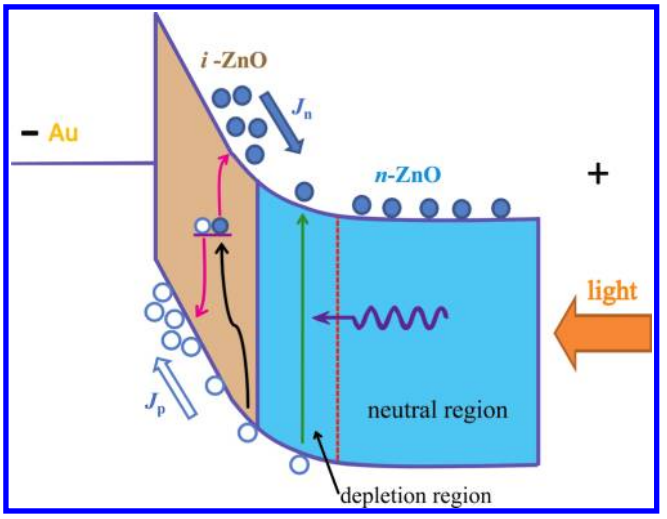

Figure 3. Schematic bandgap alignment of the i-ZnO/n-ZnO structure under reverse bias.

In this structure, the n-ZnO layer acts as a filter that makes the photodetector highly spectrum selective. Meanwhile, the i-ZnO layer will act as a "multiplier" in which an impact ionization process occurs and makes the responsivity of the photodetector greatly enhanced. In this way, a high spectrum selectivity of only 9 nm in bandwidth has been achieved, and the responsivity of the photodetectors can reach 4.91 A/W at −5 V bias, which corresponds to a quantum efficiency of as high as 1600%.

EXPERIMENTAL DETAILS

To fabricate the photodetectors, a ZnO film was first grown on an a-plane sapphire substrate using a plasma-assisted molecular beam epitaxy technique. The precursors used for the growth were elemental zinc (6 N in purity) and O_2 gas (5 N in purity). The O_2 gas was activated in an Oxford Applied Research plasma cell (model HD25) at a fixed power of 300 W. During the growth process, the substrate temperature was fixed at 750 °C and the chamber pressure at 3×10^{-5} mbar. The as-grown ZnO film has a thickness of about 350 nm and shows n-type conduction with an electron concentration of 4.2×10^{17} cm^{-3} and an electron mobility of 46 cm^2 V^{-1} s^{-1}. Then, an insulating ZnO layer, whose resistivity is too high to be measured from our Hall measurement, was deposited onto the n-ZnO layer in a radio frequency magnetron sputtering technique. For the deposition of the i-ZnO layer, a sintered ZnO (4 N in purity) ceramic target was used as the source material, and a mixed gas of oxygen and argon with a flow ratio of 5:4 was introduced into the sputtering chamber. During the deposition, the chamber pressure was maintained at 2.0 Pa; the sputtering radio frequency power was fixed at 130 W; and the substrate temperature was kept at 400 °C. In this way, the i-ZnO/n-ZnO structures have been prepared. Then, a Au layer was deposited onto the i-ZnO and an In layer onto the n-ZnO layer acting as contacts by vacuum evaporation. The electrical properties of these films and the current−voltage ($I-V$) curve of the device were characterized employing a Hall measurement system (LakeShore 7707). Both optical transmission and absorption spectra were recorded using a Shimadzu UV-3101PC spectrophotometer. The photoresponse of the photodetector was measured using a 150 W Xe lamp, monochromator, chopper (EG&G 192), and lock-in amplifier (EG&G124A) at room temperature.

RESULTS AND DISCUSSION

The inset of Figure 1 shows the structure illustration of the proposed i-ZnO/n-ZnO photodetector. The $I-V$ characteristic of the structure under dark conditions is shown in Figure 1. The curve shows a weak rectification behavior at the reverse bias region, while it is almost a beeline at the positive bias region.

The response spectrum of the photodetector under back-illumination condition at zero bias is shown in Figure 2. As shown in the figure, the response spectrum shows a predominant peak with a full width at half-maximum (fwhm) of only about 9 nm. That is, the photodetector shows response only to a very small spectrum span, which means this photodetector has a high spectrum selectivity.

To explore the origin of the high spectrum selectivity of the photodetector, the band alignment of the i-ZnO/n-ZnO structure under reverse bias (with negative voltage applied on Au contact and positive voltage on In contact) is illustrated in

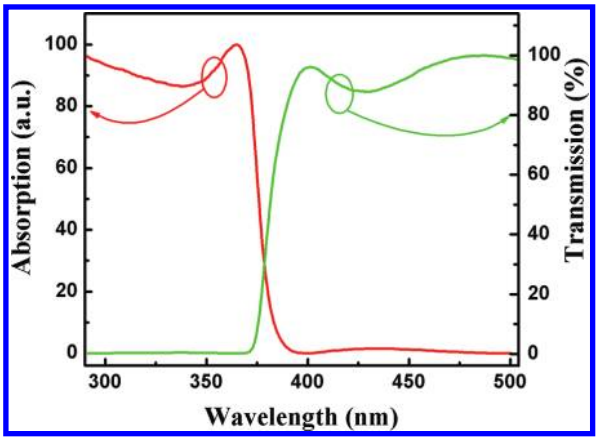

Figure 4. Transmission and absorption spectra of the *n*-ZnO layer.

Figure 3. Because of the different carrier concentration in the *i*-ZnO and *n*-ZnO layer, carriers will re-equilibrate, and a junction will form at the *i*-ZnO/*n*-ZnO interface, as evidenced by the weak rectification behavior observed in the negative bias region of the $I-V$ curve of the structure shown in Figure 1. Note that the *n*-ZnO layer can be divided into two regions: a thin space-charge region which can also be referred to as the depletion region near the *i*-ZnO and a neutral region in the *n*-ZnO layer, as depicted in Figure 3. When the illumination light passes through the neutral region of the *n*-ZnO layer, the photons with their energy larger than the bandgap of ZnO will be absorbed greatly. To depict this issue more vividly, the absorption and transmission spectra of the *n*-ZnO layer are shown in Figure 4. As evidenced from the spectra, the layer has a strong absorption to photons with wavelength shorter than 380 nm, while it is almost transparent to those with wavelength longer than 400 nm. One can then judge from the absorption and transmission spectra that when the illumination light is shed onto the structure from the *n*-ZnO side only photons with their wavelength longer than 380 nm can pass through the *n*-ZnO layer, while those with shorter wavelength will be absorbed by this layer. Since the penetration length of photons is inversely proportional to their wavelength, the shorter their wavelength is, the stronger they would be absorbed by the *n*-ZnO layer. Considering that the photogenerated carriers can contribute to the response of the photodetector only if they are separated at the *i*-ZnO and *n*-ZnO interface, as the electric field in the neutral region is weak, most of the carriers generated in the top layer of the neutral region due to the absorption of short-wavelength photons can not reach the depletion region in the time scale of their lifetime, thus they will not contribute to the photoresponse. In this way, the photons with short wavelength will be filtrated by the neutral region, and only those in a very narrow spectrum can contribute to the response of the structure. Consequently, the photodetector shows rather high spectrum selectivity.

One can speculate from the bandgap diagram of the structure that when the photogenerated holes drift toward the Au electrode they have to pass through the *i*-ZnO layer. Considering that most of the voltage will be applied onto the *i*-ZnO layer because of its large resistivity and the thickness of the *i*-ZnO is only 80 nm, the electric field in this layer will be very high; e.g., it will be as high as 6.25×10^5 V/cm at -5 V bias. Then when the photogenerated holes move into this layer, they will be accelerated by such a high electric field. Thus, some holes will gain much

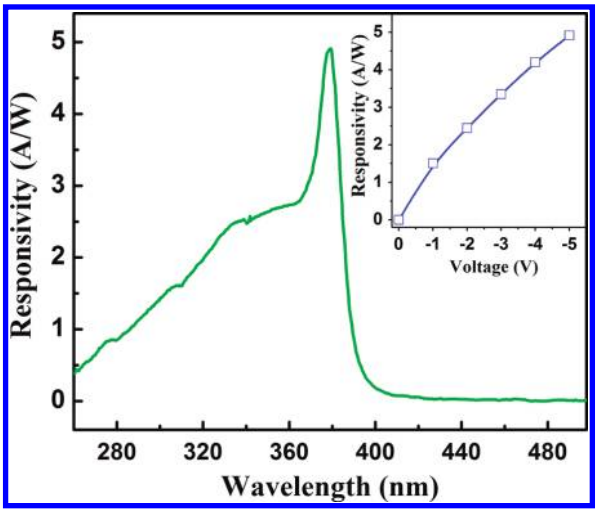

Figure 5. Response spectrum of the photodetector at -5 V bias, and the inset shows the maximum responsivity of the photodetector as a function of the applied bias.

energy, and impact with the lattice of the *i*-ZnO, and release their energy to excite additional carriers in the *i*-ZnO layer. In this way, additional carriers will be generated via the above-mentioned impact ionization process,[18,19] and then the number of carriers that can be collected by the electrodes will be increased. As a result, the responsivity of the photodetector can be greatly enhanced. To test the reasonability of the above speculation, the photoresponse features of the *i*-ZnO/*n*-ZnO structure under reverse bias have been investigated, the results of which are shown in Figure 5. The inset of Figure 5 shows the relationship between the maximum responsivity of the photodetectors and the applied bias. The responsivity increases greatly with increasing the reverse bias, and it can reach 4.91 A/W at -5 V bias. Such a relationship is reasonable because elevated bias will facilitate the impact ionization process. The quantum efficiency η of a photodetector can be given by the following formula[20]

$$\eta = \frac{I_{ph}}{q}\left(\frac{h\nu}{P_{opt}}\right) \quad (1)$$

where I_{ph} is the photogenerated current by the absorption of incident optical power P_{opt} at a wavelength λ (corresponding to a photon energy $h\nu$). The quantum efficiency of the ZnO photodetector at -5 V bias determined from eq 1 is 1600%, which reveals that there is relatively high photocurrent gain in the photodetector, confirming the above-speculated impact ionization process has indeed occurred.

Since a wider depletion region will form at higher reverse bias, the neutral region of the *n*-ZnO layer will be shortened as the applied bias is increased, which means the volume of the neutral ZnO that can act as a "filter" for the photodetector will be decreased. To confirm the effectiveness of the "filter" at higher reverse bias, the response spectrum of the structure at -5 V bias is measured and shown in Figure 5. As shown in the figure, although the response to short-wavelength photons increases, a sharp band still dominates the spectrum, indicating the selectivity of the photodetector has not been deteriorated drastically. We note that since the selectivity of the photodetector depends on the thickness of the *n*-ZnO neutral layer, at larger bias, the selectivity of the photodetector worsens because the thickness of

the "filter" layer is decreased. Nevertheless, to increase the responsivity of the photodetector, a bias has to be applied onto the structure. For practical applications, one has to make a trade-off between the selectivity and responsivity of the photodetector. If better response selectivity is needed, one can decrease the bias to realize better response selectivity, while if larger responsivity is needed, one has to increase the bias to sacrifice the selectivity. In this sense, the thickness of the *n*-ZnO layer could provide an extra degree of freedom for designing different detectors to meet various practical applications.

CONCLUSIONS

Highly spectrum-selectively ultraviolet photodetectors with high internal gain have been proposed and fabricated from *i*-ZnO/*n*-ZnO structure. In this structure, the *n*-ZnO layer acts as a "filter" that filtrates out the response of short-wavelength photons, and the *i*-ZnO layer acts as a "multiplier", in which an impact ionization process occurs to enhance the responsivity of the photodetectors greatly. A highly spectrum-selective photodetector with its response bandwidth of only 9 nm has been obtained, and by utilizing an impact ionization process, the responsivity of the photodetector can reach 4.91 A/W at −5 V bias corresponding to a quantum efficiency of around 1600%. The results reported in this paper may also be applicable to other material systems, thus may provide a general route to high-performance, high-responsivity photodetectors.

AUTHOR INFORMATION

Corresponding Author
*E-mail: phycxshan@yahoo.com.cn.

ACKNOWLEDGMENT

This work is supported by the National Basic Research Program of China (2011CB302006), the Natural Science Foundation of China (11134009, 10974197, and 11074248), and the Science and Technology Developing Project of Jilin Province (20111801).

REFERENCES

(1) Gong, X.; Tong, M. H.; Xia, Y. J.; Cai, W. Z.; Moon, J. S.; Cao, Y.; Yu, G.; Shieh, C. L.; Nilsson, B.; Heeger, A. J. *Science* **2009**, *325*, 1665.
(2) Konstantatos, G.; Sargent, E. H. *Nature Nanotechnol.* **2010**, *5*, 391.
(3) Collins, C. J.; Chowdhury, U.; Wong, M. M.; Yang, B.; Beck, A. L.; Dupuis, R. D.; Campbell, J. C. *Appl. Phys. Lett.* **2002**, *80*, 3754.
(4) Liu, K. W.; Sakurai, M.; Liao, M. Y.; Aono, M. *J. Phys. Chem. C* **2010**, *114*, 19835.
(5) Du, X. L.; Mei, Z. X.; Liu, Z. L.; Guo, Y.; Zhang, T. C.; Hou, Y. N.; Zhang, Z.; Xue, Q. K.; Kuznetsov, A. Y. *Adv. Mater.* **2009**, *21*, 4625.
(6) Cao, P.; Wang, Z. Z.; Liu, K. H.; Xu, Z.; Wang, W. L.; Bai, X. D.; Wang, E. G. *J. Mater. Chem.* **2009**, *19*, 1002.
(7) Razeghi, M.; Rogalski, A. *J. Appl. Phys.* **1996**, *79*, 7433.
(8) Jin, Y. Z.; Wang, J. P.; Sun, B. Q.; Blakesley, J. C.; Greenham, N. C. *Nano Lett.* **2008**, *8*, 1649.
(9) Look, D. C. *Mater. Sci. Eng.* **2001**, *B80*, 383.
(10) Look, D. C.; Reynolds, D. C.; Hemsky, J. W.; Jones, R. L.; Sizelove, J. R. *Appl. Phys. Lett.* **1999**, *75*, 811.
(11) Endo, H.; Sugibuchi, M.; Takahashi, K.; Goto, S.; Sugimura, S.; Hane, K.; Kashiwaba, Y. *Appl. Phys. Lett.* **2007**, *90*, 121906.
(12) Peng, S. M.; Su, Y. K.; Ji, L. W.; Wu, C. Z.; Cheng, W. B.; Chao, W. C. *J. Phys. Chem. C* **2010**, *114*, 3204.
(13) Wang, G. P.; Chu, S.; Zhan, N.; Lin, Y. Q.; Chernyak, L.; Liu, J. L. *Appl. Phys. Lett.* **2011**, *98*, 041107.
(14) Soci, C.; Zhang, A.; Xiang, B.; Dayeh, S. A.; Aplin, D. P. R.; Park, J.; Bao, X. Y.; Lo, Y. H.; Wang, D. *Nano Lett.* **2007**, *7*, 1003.
(15) Liang, S.; Sheng, H.; Liu, Y.; Huo, Z.; Lu, Y.; Shen, H. *J. Cryst. Growth* **2001**, *225*, 110.
(16) Zhu, H.; Shan, C. X.; Yao, B.; Li, B. H.; Zhang, J. Y.; Zhao, D. X.; Shen, D. Z.; Fan, X. W. *J. Phys. Chem. C* **2008**, *112*, 20546.
(17) Zhang, Z. P.; von Wenckstern, H.; Schmidt, M.; Grundmann, M. *Appl. Phys. Lett.* **2011**, *99*, 083502.
(18) Zhu, H.; Shan, C. X.; Wang, L. K.; Zheng, J.; Zhang, J. Y.; Yao, B.; Shen, D. Z. *J. Phys. Chem. C* **2010**, *114*, 7169.
(19) Wang, W. J.; Shan, C. X.; Zhu, H.; Ma, F. Y.; Shen, D. Z.; Fan, X. W.; Choy, K. L. *J. Phys. D: Appl. Phys.* **2010**, *43*, 045102.
(20) Sze, S. M. *Physics of Semiconductor Devices*, 2nd ed.; John Wiley: New York, 1981.